Synchronization of Delay-Coupled Oscillators: A Study of Semiconductor Lasers

H.-J. Wünsche,[1] S. Bauer,[2] J. Kreissl,[2] O. Ushakov,[1] N. Korneyev,[1] F. Henneberger,[1] E. Wille,[3] H. Erzgräber,[3] M. Peil,[3] W. Elsäßer,[3] and I. Fischer[3]

[1]*Institut für Physik, Humboldt-Universität zu Berlin, Newtonstrasse 15, 12489 Berlin, Germany*
[2]*Fraunhofer-Institute for Telecommunications, Heinrich-Hertz-Institut, Einsteinufer 37, 10587 Berlin, Germany*
[3]*Institute of Applied Physics, Darmstadt University of Technology, Schloßgartenstrasse 7, 64289 Darmstadt, Germany*

(Received 16 July 2004; revised manuscript received 12 January 2005; published 26 April 2005)

Two delay-coupled semiconductor lasers are studied in the regime where the coupling delay is comparable to the time scales of the internal laser oscillations. Detuning the optical frequency between the two lasers, novel delay-induced scenarios leading from optical frequency locking to successive states of periodic intensity pulsations are observed. We demonstrate and analyze these dynamical phenomena experimentally using two distinct laser configurations. A theoretical treatment reveals the universal character of our findings for delay-coupled systems.

DOI: 10.1103/PhysRevLett.94.163901 PACS numbers: 42.55.Px, 02.30.Ks, 05.45.Xt, 42.65.Sf

The concept of coupled nonlinear oscillators has proven to be extremely successful in order to understand complex systems in all fields of science. Synchronization and resonance phenomena are common features of those systems [1,2]. In recent years, the role of delay, arising from a finite propagation time of the coupling signals, has become a focus of interest. Specific implications are the occurrence of multistable synchronization [3,4], symmetry breaking [5], or amplitude death [6].

Semiconductor lasers (SLs) are ideal candidates for studying delay-coupled nonlinear oscillators. Modern processing technology allows one to build SLs with exactly defined properties. Single-mode operation up to high pump currents is generally achieved, especially for distributed feedback (DFB) lasers. The parameters relevant for the coupling like spectral detuning, coupling delay, and strength can be tuned over a wide range. The nonlinear properties of the solitary SL are well studied. Furthermore, recent studies on SLs under passive optical feedback with short delay have revealed novel dynamical scenarios [7–10] that provide a suitable starting point for elucidating the more complex case of interacting lasers.

The time scale governing the dynamics of a solitary SL is given by the period τ_{RO} of the relaxation oscillations of the carrier-photon system. This period is typically in the range of a few 100 ps. The coupling delay τ results from the propagation of the optical fields between the spatially separated lasers. In the long-delay limit $\tau \gg \tau_{\mathrm{RO}}$, a complex behavior comprising low frequency fluctuations and chaos synchronization in conjunction with symmetry breaking has been observed [5]. Here, we concentrate on the regime of short delays in order to unveil the fundamental instabilities in these systems. Two configurations of coupled DFB lasers are experimentally investigated. The free-space configuration (FSC) allows for a spatial separation of the lasers corresponding to a delay $\tau \simeq \tau_{\mathrm{RO}}$. The case of ultrashort delay $\tau \ll \tau_{\mathrm{RO}}$ is realized by an integrated tandem device (ITD) where both lasers are arranged on a single chip. We find qualitatively the same dynamics for both configurations underlining the universal nature of the observed phenomena and provide deeper insight by a theoretical analysis, comprising both a device-specific treatment as well as a generic model for delay-coupled oscillators.

A scheme of the FSC is shown in Fig. 1(a). Two device-identical 1540 nm single-mode DFB lasers grown on the same wafer have been selected. The light output of each laser is collimated, passes a 50/50 beam splitter, and is injected into its counterpart. The extracted power is used to measure the optical spectra and the intensity dynamics of both lasers. The detection branches are separated from the coupled lasers by two optical isolators. The lasers are temperature stabilized to better than 0.01 K. Their emission wavelengths under solitary operation agree within 0.05 nm, the threshold currents within 1%, and the relaxation oscillation frequencies within 5%, respectively. The linewidth enhancement factor of amplitude-phase coupling, measured according to [11], is $\alpha \approx 2$ for both SLs. The free-running frequency of each laser can be tuned by temperature variation following a linear function with -12.1 GHz/K. The optical path length $d = 51 \pm 1$ mm between the devices results in a delay of $\tau = 170 \pm 3$ ps. We estimate that a few percent of the emission power of each laser is injected into its counterpart.

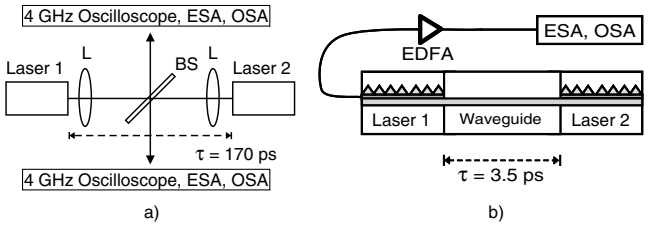

FIG. 1. Schemes of experimental setups. (a) Free-space configuration; (b) integrated tandem device. ESA: electrical spectrum analyzer; OSA: optical spectrum analyzer; BS: beam splitter; L: lens; EDFA: erbium doped fiber amplifier.

The ITD consists of two DFB lasers, each 220 μm long, separated by a 300 μm long passive waveguide section [Fig. 1(b)]. The coupling in the ITD is distinctly stronger, as about 50% of the field intensity passes the passive section. Irrespective of the stronger interaction, owing to a specific grating design, both lasers of the tandem operate always single mode. Current induced heating changes the refractive index in the device sections. Thus, the emission wavelengths of the lasers can be selectively detuned by asymmetric current pumping. The length of the passive section defines a delay of only $\tau \approx 3.5$ ps.

We have systematically studied the emission properties of the coupled system as a function of the spectral detuning Δf between the lasers. In the FSC, described first, great care has been taken to verify that the phenomena discussed below are due to coupling and not due to passive reflections. The lasers are pumped at 60 mA, being 6.5 times the threshold current. For these conditions, the frequency of relaxation oscillations is extrapolated to be about 15 GHz. The temperature of one laser—in the following denoted as the detuned laser—is changed in small steps covering a range of $-20 \leq \Delta f \leq 20$ GHz. The width of each step is 330 ± 90 MHz which gives the resolution of the detuning. The other laser—in the following called the stationary laser—is kept at constant temperature. For each detuning step, optical spectra of both lasers, as well as the power spectrum of the detuned laser have been recorded simultaneously. The data—summarized in Fig. 2—reveal two regimes of operation. For small detuning (-4.1 GHz $< \Delta f < 7.0$ GHz), the lasers lock onto a common optical frequency. In this regime, the emission is stable. We observe locking on three different modes of the coupled laser system. In the second regime, the lasers unlock. For large detuning, the stationary laser emits on its free-running frequency. The optical frequency of the detuned laser behaves discontinuously and follows a staircase with a slope close to the nominal detuning. In the range $|\Delta f| \gtrsim 10$ GHz, the average spectral separation between adjacent steps of 2.8 ± 0.4 GHz agrees very well with the round-trip frequency $1/2\tau = 2.9 \pm 0.1$ GHz. For smaller detuning, this separation decreases to 1.7 GHz. In Fig. 2, the detuning was continuously varied from negative to positive.

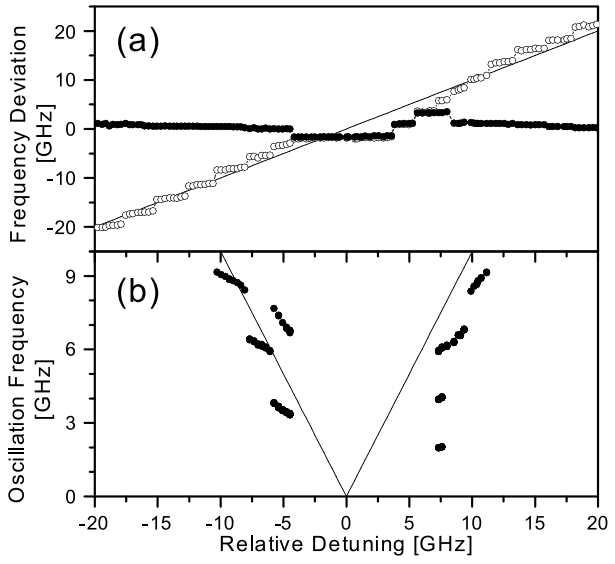

FIG. 2. (a) Dominant optical emission frequency of the stationary (●) and detuned (○) laser versus detuning of the free-running lasers for the FSC. Frequency deviations are given relative to the frequency of the free-running stationary laser. (b) Corresponding intensity oscillation frequencies taken from the power spectra. Both lasers are pumped at 60 mA. The nominal detuning is given by straight lines for comparison.

In the unlocked regime, the output of both lasers oscillates periodically. The peaks occurring in the power spectra are equal to the spectral separation of the optical emission frequencies (see Fig. 2). Two detuned oscillators would also give rise to periodic intensity modulations in the absence of delay, however, without the characteristic staircase discontinuities. Moreover, the presence of higher harmonics in the power spectra signifies that the oscillations are anharmonic, excluding also simple linear beating as the origin. Time series taken on the first stair in the unlocked regime uncover a characteristic phase shift between stationary and detuned laser depending on their detuning. As seen in Fig. 3, the phase difference changes continuously from about zero to π from one end of the stair to the other. This finding is indicative of a mode change when jumping from one stair to the next.

The ITD exhibits qualitatively the same behavior. On the stationary laser section, the pump current is fixed, while the bias on the detuned laser is increased in steps of 0.5 mA. Except for small current ranges, two sharp peaks dominate the optical spectrum [Fig. 4(a)]. The second peak appears already at about 18 mA, i.e., below the 25 mA solitary threshold, owing to optical pumping by the other laser. Whether the synchronization at smaller biases is frequency

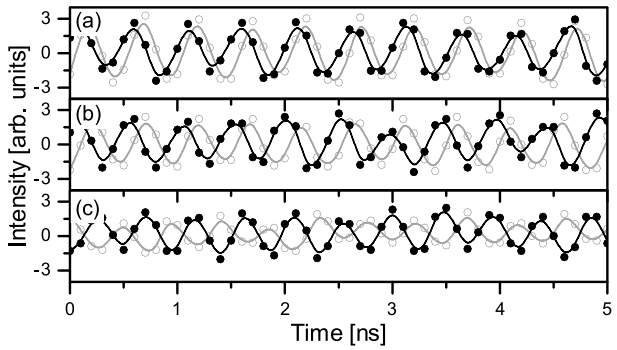

FIG. 3. Time series of the detuned (○) and stationary (●) laser, simultaneously taken for increasing detuning Δf of (a) 6.9 GHz, (b) 7.7 GHz, and (c) 8.5 GHz. Corresponding B-splines are plotted as continuous lines. The oscillation frequency is 2 GHz.

locking or caused by switching off one laser could not be distinguished experimentally. The overall shift of 2.2 nm seen for the detuned laser is consistent with that of solitary lasers from the same wafer. The peak associated with the stationary laser also moves slightly due to thermal cross talk. We emphasize that both emission lines have comparable strength although the spectrum is recorded from only one side of the tandem. Thus, the field of each laser propagates to the opposite facet without significant attenuation. The resultant intensity oscillations are hence more pronounced than in the FSC. Their frequencies monitored by the power spectra and the line separations in the optical spectra agree within the 50 GHz bandwidth of the ESA [Fig. 4(b)]. The step separation in the optical spectra are again close to the round-trip frequency of $1/2\tau \approx$ 140 GHz defined by the passive section. We conclude that discontinuities of this kind are a common feature of mutually interacting lasers with short delay.

Multistability has been predicted as a general consequence of delay for the phase-synchronization of weakly coupled oscillators [3,4]. However, the regime where the oscillators unlock has not yet been elucidated. In our subsequent theoretical analysis, we present first a specific treatment for lasers, followed by a study of two delay-coupled phase oscillators, demonstrating the universal character of the above observations.

Each DFB laser is treated within the well elaborated frame of the traveling-wave equations complemented by rate equations for the carrier density (see, e.g., [10]). The optical fields of the lasers, both operating above threshold, are related by

$$E_k^{\text{in}}(t) = KE_{k'}^{\text{out}}(t-\tau). \tag{1}$$

The complex coupling constant K incorporates attenuation and phase shift of the amplitude E_k^{in} injected in laser $k = 1, 2$ relative to the field $E_{k'}^{\text{out}}$ emitted from the opposing edge of the other laser $k' = 3 - k$. A numerical solution for the parameters of the FSC is depicted in Figs. 5(a) and 5(b). The main features of the experiment—synchronization close to zero detuning as well as the staircase structure for larger detuning—are, indeed, well reproduced. Also multistable locking on different cavity modes appears similar to Fig. 2(a). In contrast, the scenario without delay is rather conventional: the two frequencies behave continuously and their splitting increases square-root-like when synchronization is lost.

The cavity modes of Fig. 5(a) and 5(b) are calculated by using time-averaged carrier densities. Obviously, these average-cavity modes dictate the stair positions, even though the density exhibits considerable dynamics in the beating regime. At each laser facet, input and output fields associated with a compound-cavity mode of frequency ω are related by

$$q_k(\omega)E_k^{\text{out}}(\omega) = E_k^{\text{in}}(\omega). \tag{2}$$

The DFB enters by its inverse amplitude reflectivity q_k [9]. Without coupling, $q_1 = q_2 = 0$ determines the thresholds of the solitary lasers. For weak coupling, q_k can be linearized. Combining Eqs. (1) and (2) yields then the characteristic equation

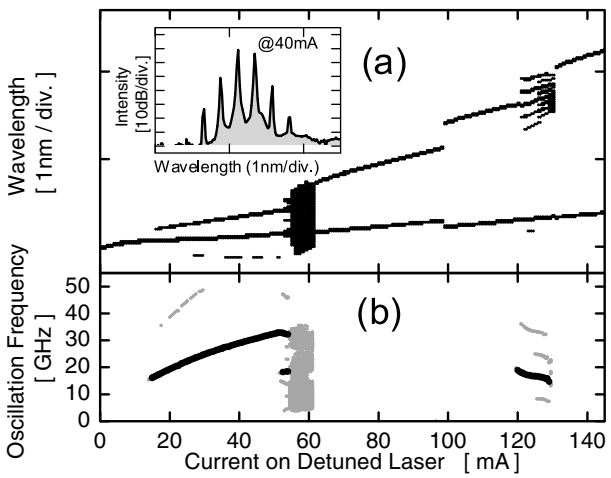

FIG. 4. Detuning scenario of the ITD. (a) Dominant lines ($\geq$ 20 dB down of the maximum peak) in the optical spectrum and their shift as a function of the pump current on the detuned laser. Inset: Optical spectrum at 40 mA. (b) Lines in the power spectrum. Black: 25 dB above noise floor; gray: side peaks more than 5 dB above noise floor. The pump current on the stationary laser is always 45 mA.

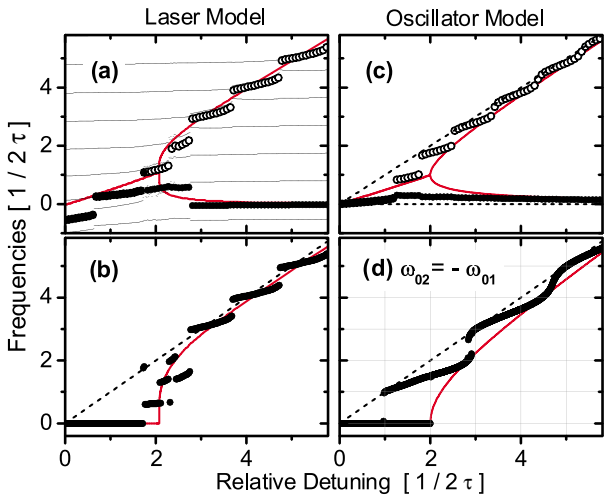

FIG. 5 (color online). Numerically calculated synchronization scenarios. All frequencies are in units of $1/2\tau$ (●, ○ as in Fig. 2). Solid gray (red): delay-free limit. Dashed line: $K = 0$. (a),(b) Lasers (FSC) ($\tau = 150$ ps, $|K|^2 = 0.1$, $\arg K = 0.6\pi$, $\alpha = 2$). (a) Optical frequencies; thin line: average-cavity modes. (b) Main peaks in power spectrum of detuned laser. (c),(d) Phase oscillators ($K\tau = \pi$), (c) Frequencies for asymmetric and (d) frequency difference for symmetric detuning.

$$\prod_{k=1,2}[\omega - \omega_{0k} + (i-\alpha)G_k] = (e^{-i\omega\tau}\kappa)^2, \qquad (3)$$

where ω_{0k} denote the eigenfrequencies of the uncoupled system and G_k are the mean gain deviations from the solitary thresholds. The coupling rate $\kappa = K/\partial_\omega q_k$ combines internal and external feedback. If the detuning is large compared to κ, there exists a pair of real solutions (Ω_1, G_1) and (Ω_2, G_2), $\Omega_k = \omega_k - \omega_{0k}$, obeying in lowest order of κ

$$\Omega_k + (i-\alpha)G_k = e^{-2i\Omega_k\tau}\eta_k, \qquad (4)$$

with $\eta_k = e^{-2i\omega_{0k}\tau}\kappa^2/(\omega_{0k} - \omega_{0k'})$. On a certain stair, two modes of the compound cavity are close to threshold and give rise to intensity oscillations. At the stair edge, the frequency-gain constellation becomes unstable and a jump to the next mode pair occurs. The feedback phase $\arg\eta_2 = -2\omega_{02}\tau$ of the detuned laser is changed by 2π within the tuning range of one round-trip frequency, consistent with the experimentally observed step separation. With the linearized q_k, Eqs. (1) and (2) yield $\Delta\varphi = -(\omega_{01} + \omega_{02})\tau$ for the phase shift between the pulsations of the lasers. This quantity, again in full accord with the experimental data, changes by π across one stair. The structure of Eq. (4) is reminiscent of that of a single laser subjected to external optical feedback [8]. The total device undergoes, indeed, a self-organization in such a way that each laser acts as a feedback element for its counterpart. A single feedback laser, however, would operate continuous wave at the coupling strengths of the present configurations. The dynamical instabilities are therefore crucially correlated with the active character of the oscillators involved.

The findings reported above reveal, in fact, the fundamental synchronization scenario under delay coupling. To demonstrate this, we consider finally the generic case of two phase oscillators $k = 1, 2$

$$\dot{\varphi}_k = \omega_{0k} - K\sin(\varphi_k - \varphi_{k'}^\tau) \qquad (k' = 3-k), \qquad (5)$$

with $\varphi_{k'}^\tau = \varphi_{k'}(t-\tau)$ [3]. The coupling term is the same as for the phase coupling of optical fields, while an internal nonlinearity is absent ($G_k = 0$). Numerical integration yields asymptotically periodic solutions. Strikingly, as seen in Figs. 5(c) and 5(d), their frequencies exhibit qualitatively the same detuning characteristics as the lasers. Particularly instructive is the case of symmetric detuning $\omega_{02} = -\omega_{01} = \Delta/2$, where all solutions examined numerically obey $\varphi_2(t) + \varphi_1(t) = \text{const}$. Making this ansatz, the closed equation

$$\dot{\phi} = \Delta - K[\sin(\phi) + \sin(\phi^\tau)] \qquad (6)$$

follows for $\phi = \varphi_2 + \varphi_2^\tau$, which generalizes the delay-free Adler equation [1]. Solutions with frequencies being integer multiples of $1/2\tau$ define representative points in the system dynamics. Here, because of $\phi = \phi^\tau + m\pi$, the coupling for ϕ (not φ_k) is either zero (m odd) or delay-free (m even). With increasing Δ, the system meanders between those limits [Fig. 5(d)]. Branches with a negative slope are unstable, providing the staircase feature. It is exactly this kind of self-organization in the phase relation between the oscillators that governs the synchronization. For lasers, the phase dynamics translates into mode changes. In addition, the internal carrier nonlinearities give rise to an extra, more complex amplitude dynamics.

In conclusion, we have reported on multistable synchronization and self-sustained amplitude pulsations with staircase-type discontinuities of two interacting oscillators. These phenomena are generated through the conjuncture of coupling delay, detuning, and nonlinearity. We have typified this for two representative nonlinear systems, the field-inversion system of lasers, and two limit-cycle oscillators. Many other interesting observations, among them hysteresis and chaotic behavior, deserve further investigations.

Part of this work was supported by the Deutsche Forschungsgemeinschaft in the frame of SFB 555. The authors thank Bernd Sartorius for providing the ITD, Nortel Networks for the DFB lasers of the FSC, Mindaugas Radziunas for using his program suite LDSL, and S. Yanchuk for letting us know his results on coupled Roessler oscillators.

[1] A. Pikovsky, M. Rosenblum, and J. Kurths, *Synchronization: A Universal Concept in Nonlinear Sciences* (Cambridge University Press, Cambridge, 2003).
[2] S. Boccaletti, L. M. Pecora, and A. Pelaez, Phys. Rev. E **63**, 066219 (2001).
[3] H. Schuster and P. Wagner, Prog. Theor. Phys. **81**, 939 (1989).
[4] S. Kim, S. H. Park, and C. S. Ryu, Phys. Rev. Lett. **79**, 2911 (1997).
[5] T. Heil *et al.*, Phys. Rev. Lett. **86**, 795 (2001).
[6] D. V. R. Reddy, A. Sen, and G. L. Johnston, Phys. Rev. Lett. **80**, 5109 (1998).
[7] T. Heil *et al.*, Phys. Rev. Lett. **87**, 243901 (2001).
[8] T. Heil *et al.*, Phys. Rev. E **67**, 066214 (2003).
[9] O. Ushakov *et al.*, Phys. Rev. Lett. **92**, 043902 (2004).
[10] S. Bauer *et al.*, Phys. Rev. E **69**, 016206 (2004).
[11] I. D. Henning and J. V. Collins, Electron. Lett. **19**, 927 (1983).